Regional Studies in Marine Science 93 (2026) 104743

Contents lists available at ScienceDirect

Regional Studies in Marine Science

journal homepage: www.elsevier.com/locate/rsma

# Age, growth, and trophic ecology of two deep-sea fish *Diaphus watasei* and *Synagrops japonicus* in the East China Sea

Dorine Ngo Nola Mara [a], David Mboglen [a,d], Luhao Fan [a], Yunkai Li [a,b,c,*]

[a] College of Marine Living Resource Sciences and Management, Shanghai Ocean University, Shanghai, China
[b] The key Laboratory of Sustainable Exploitation of Oceanic Fisheries Resources, Ministry of Education, Shanghai, China
[c] National Engineering Research Centre for Oceanic Fisheries, Shanghai Ocean University, Shanghai, China
[d] Agricultural Research Institute for Development (IRAD), Specialized Research Station on Marine Ecosystems, Ebodjé Field Station, 219, Kribi, Cameroon

ARTICLE INFO

*Keywords:*
Ontogenetic trophic shift
Intraguild predation
Stomach content analysis
Stable isotope analysis
Mesopelagic fish
East China Sea

ABSTRACT

Mesopelagic fishes are critical components of oceanic food webs, yet they face increasing pressure from emerging fisheries. This study examines the role of ontogenetic and trophic strategies in the coexistence of two predominant deep-sea fish species in the East China Sea (ECS): the lanternfish *Diaphus watasei* and the lanternbelly *Synagrops japonicus*. Using an integrative framework combining otolith microstructure, stomach content analysis (SCA), and stable isotope analysis (SIA), we reconstructed growth trajectories and ontogenetic trophic shifts. Results revealed distinct life-history strategies: *D. watasei* exhibited near-isometric growth (b = 3.07), while *S. japonicus* displayed negative allometric growth (b = 2.79), with ages ranging from 130 to 670 days and 190–640 days, respectively. Unlike previous reports of similar trophic habits between juvenile and adult stages, both species demonstrated significant ontogenetic dietary shifts. *Diaphus watasei* transitioned toward higher trophic positions characterized by increased piscivory, while *S. japonicus* exhibited a marked shift from benthic invertebrates in juveniles to benthopelagic foraging in adults. SIA confirmed clear niche segregation in juveniles but substantial isotopic overlap in adults. Crucially, this adult convergence is not solely due to competition but is driven by asymmetrical trophic dependence, as adult *S. japonicus* incorporates *D. watasei* as a key prey resource. These findings suggest that coexistence is mediated by a combination of spatial partitioning in early life stages and intraguild predation in adulthood, providing a vital baseline for predicting the ecological impacts of fisheries expansion in the ECS.

## 1. Introduction

Over the past two decades, the exploitation of deep-sea fishery resources, including those located beyond areas of national jurisdiction (ABNJ), has expanded markedly at the global scale, despite evidence that only 29 % of fish stocks are currently harvested in a sustainable manner (Morato, 2006; Bensch, 2009; Sharma et al., 2025). Among deep-sea organisms, mesopelagic fishes represent the largest vertebrate biomass in the ocean and occupy a central position in marine food webs and biogeochemical cycles (Wang et al., 2019; Iglesias et al., 2023; Rayegani, 2024). In recent years, declining coastal and shelf stocks and the persistent intensification of fishing activities have increased the commercial interest in mesopelagic organisms as potential substitute resources (Cadul et al., 2011; Grimaldo et al., 2020; Quang et al., 2024). Although these species are not yet widely exploited, their high biomass and ecological importance raise concerns regarding the potential consequences of future large-scale harvests (Kourantidou andand Jin, 2022; Prellezo et al., 2024). Understanding their trophic ecology, life-history strategies, and interspecific interactions is therefore essential to anticipate how emerging fisheries may alter deep-sea ecosystems.

The East China Sea (ECS) is among the most biologically productive yet heavily exploited marine regions worldwide (Li and Zhang, 2012; Zhang et al., 2016; Wang et al., 2024). China has been the world's largest marine fish producer since 1989, with the ECS alone contributing nearly 20 % of the total national landings (FAO, 2014). In this multispecies fishery system, mesopelagic and bathypelagic organisms constitute a substantial and recurrent component of the by-catch from commercial bottom trawling operations (Sheng and Cheng, 1989; Ohshimo et al., 2012; Sassa et al., 2016). Although these species are generally considered of low commercial value and are not currently

* Corresponding author at: College of Marine Living Resource Sciences and Management, Shanghai Ocean University, Shanghai, China.
*E-mail address:* ykli@shou.edu.cn (Y. Li).

https://doi.org/10.1016/j.rsma.2025.104743
Received 9 September 2025; Received in revised form 19 December 2025; Accepted 29 December 2025
Available online 3 January 2026

targeted directly, the magnitude and persistence of their by-catch suggest increasing interactions with fishing activities, and potentially growing exploitation interest as traditional stocks decline (Cheng et al., 2009; Pauly et al., 2021). Their removal may have disproportionate ecological consequences due to their role in mediating energy transfer between epipelagic, mesopelagic, and benthopelagic compartments.

Among the species frequently encountered in ECS by-catch, the lanternfish *Diaphus watasei* (Myctophidae) and *Synagrops japonicus* (Acropomatidae) are of ecological relevance. Both species contribute substantially to the regional food web (Sassa et al., 2010; Ohshimo et al., 2012; Chen et al., 2025), yet their ecological significance remains poorly understood. Previous studies have shown that adults of both species occupy similar trophic positions based on stable isotope analysis (Chen et al., 2025), despite their contrasting diet compositions. *Diaphus watasei*, a vertical migrator, is predominantly piscivorous and feeds largely on mesopelagic teleosts such as *Maurolicus muelleri*. In contrast, *S. japonicus*, likely a weak or non-migrant, displays a broader feeding strategy that includes both benthic invertebrates and mesopelagic fishes, notably species of *Diaphus spp* (Ozawa and Zinno, 1990; Sassa et al., 2016; Serena et al., 2022; Wang et al., 2019). Their coexistence is further shaped by life-stage-specific vertical migration patterns: juveniles and immature *D. watasei* undertake diel vertical migrations into epipelagic layers at night, while adults remain largely in deeper waters where they overlap more extensively with *S. japonicus* (Gartner et al., 1997; Sassa et al., 2016; Eduardo et al., 2024; Chen et al., 2025).

These ontogenetic shifts in vertical distribution and prey use suggest that trophic interactions between the two species may be more complex than simple resource partitioning (Ross, 1986; Varghese et al., 2014; Eduardo et al., 2020). The regular occurrence of *D. watasei* in the diet of *S. japonicus* raises the possibility of an asymmetric trophic relationship (Polis et al., 1989), where the latter despite its generalist feeding strategy relies on *D. watasei* as a predictable mesopelagic prey resource linking benthic and pelagic food webs (Trueman et al., 2014; Drazen and Sutton, 2017). Testing this hypothesis requires not only documenting dietary patterns but also linking them to growth trajectories and ontogenetic transitions that govern habitat use and prey availability. In this context, otolith microstructure analysis provides key insights into age, growth, and life-history shifts, enabling the identification of size- and age-dependent transitions that can structure trophic interactions and influence vulnerability to predation (Sogard, 1997; Gagliano et al., 2007). Size–weight relationships and otolith morphometrics further allow the detection of phenotypic variations that may be associated with ecological strategies, such as foraging behavior, vertical movement capacities, and life-history pacing traits directly relevant to predator–prey dynamics (Tuset et al., 2003; Lombarte and Cruz, 2007).

Given this complex interplay of life-history and trophic strategies, their partial spatial overlap, comparable trophic positions, and shared reliance on mesopelagic prey have led several authors to consider potential competitive interactions within multispecies mesopelagic assemblages (Sassa et al., 2016; Chen et al., 2025). In the ECS, such overlap is expected to be further intensified by the cumulative removal of higher-trophic predators and the progressive “fishing down” of the food web (Liang and Pauly, 2017; Szuwalski et al., 2017), which can increase competition among mid-trophic-level consumers. Here, we do not assume that competition necessarily occurs between *D. watasei* and *S. japonicus* but instead treat it as a plausible ecological mechanism that may influence their coexistence. Clarifying whether these species coexist primarily through resource partitioning, symmetric competition, or an asymmetric predator–prey relationship is therefore essential to understanding the trophic functioning of mesopelagic communities under increasing fishing pressure.

Therefore, the main objective of this study is to test the hypothesis that the coexistence of *D. watasei* and *S. japonicus* in the ECS is mediated not only by interspecific resource partitioning but also by an asymmetric trophic dependency, in which S. japonicus incorporates *D. watasei* as a key prey resource. To achieve this objective, we used an integrative framework combining: (1) otolith microstructure and morphometric analyses to reconstruct growth trajectories and identify major life-history transitions; (2) stomach content analysis (SCA) to document direct feeding relationships and ontogenetic diet shifts; and (3) stable isotope analysis (SIA) of carbon ($\delta^{13}C$) and nitrogen ($\delta^{15}N$) to quantify trophic positions and long-term resource use. This combined approach allows us to (i) assess the trophic interaction and potential dependency between *S. japonicus* and *D. watasei* across life stages, (ii) determine how growth and ontogenetic habitat shifts shape trophic niches, and (iii) evaluate the relative contributions of resource partitioning and asymmetric trophic relationships to the coexistence of these two species in the deep-sea ecosystem of the East China.

## 2. Materials and methods

### 2.1. Sample collection

The samples of *D. watasei* and *S. japonicus* were obtained as bycatch from the commercial bottom trawl fisheries at four stations in the ECS during two sampling periods: February to April 2023 and April 2024 (Fig. 1). The trawling operations were conducted at depths ranging from 300 and 400 m, using nets with a mesh size of 40 mm, primarily targeting demersal species. After collection, the samples were sorted and then stored at −20 °C for further analysis.

### 2.2. Morphometric measurements

In the laboratory, the specimens were visually identified and, when necessary, confirmed using DNA barcoding technology. Then standard length (SL ± 0.01 mm) and body weight (W ± 0.01 g) (0.1 g in a few cases) were measured. Life stages (adult or juvenile) for *S. japonicus* were determined based on the presence, absence, or condition of the gonads following the MEDITS protocol (Relini, 2015). This evaluation relied on key morphological criteria, including the appearance of the ovarian tunic, testis length, and the presence of free spermatozoa. The mean length at maturity for this species was established at 110 mm. In contrast, individuals of *D. watasei* were classified as juveniles when their standard length was below 120 mm, based on the known size at maturity for this species in the ECS (Sassa et al., 2016). Sagittal otoliths of each specimen were extracted, carefully cleaned of any soft tissue, air-dried at room temperature, and subsequently examined under an optical microscope (Olympus U-TVO.63XC) equipped with a digital camera connected to a computer. Otolith length (OL) and width (OW) were measured with a precision of ± 0.01 mm using Digimizer image analysis software and embedded in epoxy resin, placed in appropriate molds, and left to harden for 24 h. Polishing was performed using a Struers LaboPol-6 polishing unit with abrasive papers of varying grits sizes dependent on the species: 600, 1200, and 3000 grit for *Diaphus watasei*, and 600, 1200, and 2500 grit for *S. japonicus* otoliths respectively. Micro-increments were observed using an OLYMPUS CX23 optical microscope equipped with a digital camera. Visualization and increment count were conducted using FCsnap software. Each otolith was read twice, from the core to the outer edge and then in the reverse; when no significant difference was observed between readings (paired *t*-test, $p > 0.05$), the average count was used, following the methodology outlined by Campana and Jones (1992) and Tomás and Panfili, (2000). Age (in days) was estimated based on the number of daily growth increments, and age–length growth was modeled using non-linear growth functions, including the von Bertalanffy, Gompertz, and Logistic models, following standard fish growth modeling approaches (Cailliet et al., 2006).

### 2.3. Stomach content analysis

Stomachs were dissected, and their contents preserved in 70 % ethanol. Prey items were examined and counted under a stereoscopic

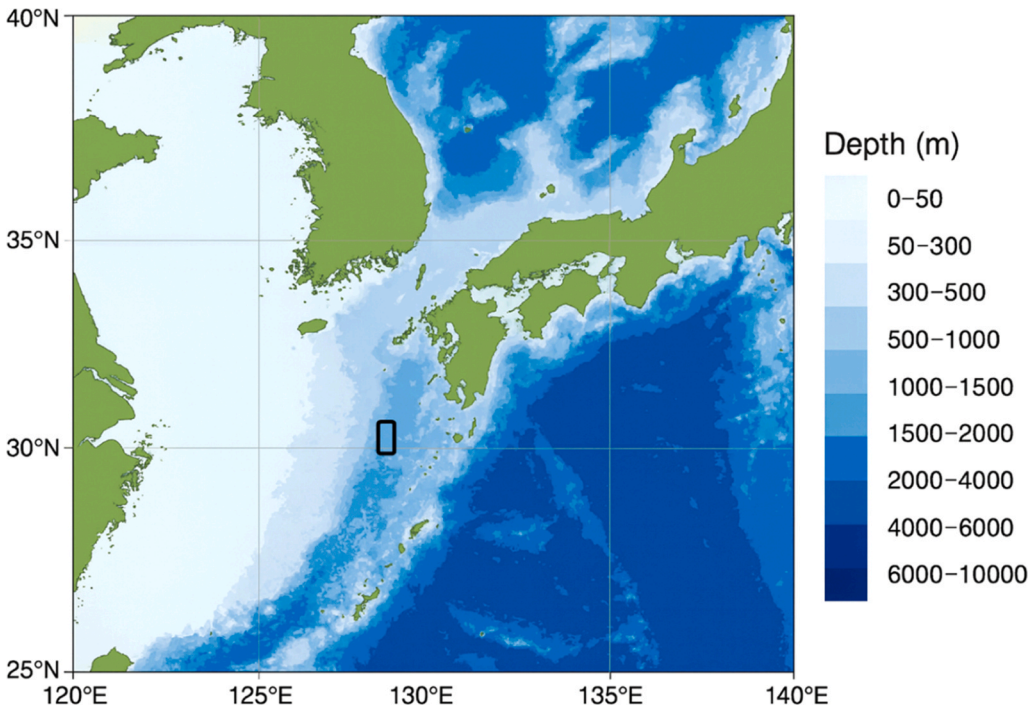


**Fig. 1.** Map of the sampling area. The black rectangle indicates the collection zone.

microscope, weighed to nearest 0.01 mg, and identified to the lowest possible taxonomic level depending on their state of digestion. The prey preference was determined through the prey-specific index of relative importance (%PSIRI):

$$PSIRI = \frac{\%FOi(\%PNi + \%PWi)}{2} \quad (1)$$

Where %PNi is the prey-specific abundance by counts, %PWi the prey-specific abundance by weights, and %FOi the frequency of occurrence (Brown et al., 2012). Unlike the traditional compound IRI, the %PSIRI was selected for its additive properties and its ability to prevent the overestimation of rare but voluminous prey, offering a more robust estimation of dietary importance across taxonomic levels. The vacuity index (VI) was calculated using the following formula: VI (%) = (A × / B, where A is the number of empty stomachs and B is the total number of stomachs examined (Hyslop, 1980).

### 2.4. Carbon ($\delta^{13}C$) and Nitrogen ($\delta^{15}N$) isotopes analysis

Stable isotopes analysis was performed on dorsal white muscle tissue (without skin) obtained from 97 fish. Each sample was rinsed with ultrapure water, freeze-dried at −55°C for 36 h, and then homogenized into a fine powder using a freeze mixer ball mill. Lipids were extracted from the samples (~1.5 mg) according to the method of Li et al. (2016). Briefly, 12 mL of a chloroform: methanol solution (2:1, v/v) was added, and the mixture was vigorously vortexed and incubated for 24 h. Following centrifugation, the supernatant was collected, and the remaining sample was dried in an oven at 40 °C. The resulting defatted powder (~1.5 mg) was then encapsulated in a tin capsule for subsequent analysis. $\delta^{13}C$ and $\delta^{15}N$ values were determined using a Vario ISOTOPE cube elemental analyzer (Germany), coupled with a continuous flow IsoPrime 100 mass spectrometer (United Kingdom), the results are expressed using delta notation (δX, in ‰), according to the following equation:

$$\delta X = \left[\left(R_{sample} - R_{standard}\right) - 1\right] \times 1000 \quad (2)$$

where X is $\delta^{13}C$ or $\delta^{15}N$, $R_{sample}$ is the isotopic ratio between ($^{13}C/^{12}C$ and $^{15}N/^{14}N$), and $R_{standard}$ is the international standard.

To validate the precision and accuracy of the isotopic measurements, laboratory internal standards (protein: $\delta^{13}C = -26.98$ ‰, $\delta^{15}N = 5.96$ ‰) were analyzed in triplicate within each batch of 15 unknown samples. Instrumental calibration was performed against the international reference materials USGS 24 (−16.5 ‰, relative to VPDB) for carbon and USGS 26 (+53.7 ‰, relative to $N_2$) for nitrogen. This calibration procedure ensured measurement uncertainties of ±0.20 ‰ for $\delta^{1}{}^{3}C$ and $\delta^{1}{}^{5}N$.

Isotopic measurements were carried out at the Key Laboratory of Sustainable Exploitation of Pelagic Fishery Resources, Ministry of Education, at Shanghai Ocean University.

### 2.5. Data analysis

The allometric growth of the organisms was modeled to define discrete life stages for subsequent analysis of trophic shifts. The relationship between standard length (SL) and weight (W) was expressed by the power function $W = aL^b$. This equation was linearized as $\log(W) = \log(a) + b\log(L)$and the parameters $a$(the intercept) and $b$(the slope, or allometric coefficient) were estimated using an ordinary least squares (OLS) regression (Le Cren, 1951). To account for the snapshot nature of stomach content (SCA) data, the species were subdivided into life stages for dietary analysis. For each species, designated here as consumers (*D. watasei* adults, *D. watasei* juveniles, *S. japonicus* adults and *S. japonicus* juvenile). We used an iterative, randomised procedure to determine the sufficiency of the sample size for dietary characterisation. The representativeness of the collected stomachs was evaluated by cumulative prey diversity curves, which plotted the progressive increase in trophic diversity against the number of stomachs. The process involved 1000 randomisations of the stomach analysis sequence for each designated group, from which a mean diversity curve was derived using the Shannon index (H′). According to Alonso et al. (2002), sample size was considered adequate when the asymptote of the mean diversity curve was reached. This stabilisation point was identified as the number of samples after which at least two consecutive points on the curve stayed within a ± 5 % range of the overall trophic diversity calculated for all

the samples.

The stomach contents were tested to determine whether diet compositions differed among consumers. An initial PERMDISP test revealed significant heterogeneity in multivariate dispersions ($F = 249.75$, $p < 0.001$); a one-way permutational multivariate analysis of variance (PERMANOVA) to a matrix derived from square-root transformed of preys abundance data (at the species taxonomic level) using Bray-Curtis similarity matrices with 9999 permutations were applied. If significant results were found ($p < 0.05$), post hoc analyses (pairwise comparisons) were applied to identify specific differences between consumers. To explore the structure of predator–prey relationships, a principal component analysis (PCA) was performed based on the cumulative abundance of each prey category found in consumer stomachs. Principal components were extracted by using the correlations among cumulative prey as variables and PCA plots were used to visualise the trophic interaction among consumers with highly correlated (Pearson correlation > 0.5) prey.

The trophic niche dimensions for the consumers were quantified using metrics derived from both SCA and SIA. From the SCA data, the standardized Levin index ($B_{STA}$) was used to evaluate the diet breadth (Krebs 1999):

$$B_{sta} = \frac{1}{n-1}\left(\frac{1}{\sum_j Pij^2} - 1\right), \quad (3)$$

where $Pij$ = proportion of the diet of consumer $i$ on prey $j$, and n = total number of prey categories. $B_{STA}$ values were interpreted as indicating narrow to broad diet breadth (Krebs, 1999). The Pianka niche index (Pianka, 1973) was used to determine the diet overlap among the different consumers, as:

$$O_{ik} = \frac{\sum_i^n P_{ij} \quad P_{ik}}{\sqrt{\sum_i^n P_{ij}^2 \sum_i^n P_{ik}^2}}, \quad (4)$$

Where $O_{jk}$ = Pianka's measure of niche overlap between species $j$ and species $k$, $P_{ij}$ = Proportion resource $i$ is of the total resources used by species $j$; $Pik$ = Proportion resource $i$ is of the total resources used by species $k$, and $n$ = Total number of prey categories. A key characteristic of this latter metric is its symmetrical nature, wherein the calculated overlap from consumer A to consumer B is identical to that from consumer B to consumer A. The index yields values bounded between 0 (no overlap) to 1 indicating (total overlap). The resulting overlap values were categorised as low (0–0.39), intermediate (0.4–0.6), or high (0.61–1) according to Grossman and Hart (1986). The unidentified fish group was excluded from these analyses.

The isotopic tracers $\delta^{13}C$ and $\delta^{15}N$, were used to quantify the isotopic niche size and overlap among the consumers using a Bayesian framework NicheROVER (Swanson et al., 2015). This approach generates probabilistic estimates of niche region by calculating the proportion of the posterior distribution of one consumer's niche region (e.g., juvenile *D. watasei*) that is contained within that of a second consumer (e.g., juvenile *S. japonicus*). Niche overlap was calculated from 1000 Monte Carlo draws with an alpha = 0.95 probability level and is defined as the probability of finding a consumer from one group in the Isotopic niche regions ($N_R$) of another consumer group.

Trophic levels of each consumer group were estimated through the prey found in the stomachs ($TP_{sca}$) and the values of the isotopic tracers ($TP_{Consumer}$). $TP_{SCA} = 1 + \left(\sum_{j=1}^{n} P_j * TL_j\right)$, where $TL_{SCA}$ is the trophic level of the consumer, $P_j$ is the proportion of each prey category in the stomach (W %), and $TL_j$ is the trophic level of each prey category $j$. $TL_j$ were obtained from Chen et al. (2025) and the information registered in Fishbase (www.fishbase.org).

$TP_{Consumer} = \frac{\left(\delta^{15}N_{Consumer} - \delta^{15}N_{baseline}\right)}{\Delta^{15}N} + \lambda$, where $\delta^{15}N_{Consumer}$ is the value for the consumers, $\delta^{15}N$baseline = 7.73 ‰, $\Delta^{15}N = 3.4$ ‰ and $\lambda = 2$ according to Zou et al. (2022).

Prior to analysis, the assumptions of normality and homogeneity of variances were verified. The distribution of residuals was assessed for normality using Q-Q plots and the Shapiro-Wilk test, while homogeneity of variances was checked using Levene's test. Based on these diagnostic checks, differences in isotopic values ($\delta^{13}C$ and $\delta^{15}N$) between consumer groups were tested using either a one-way ANOVA or a Kruskal-Wallis test (when one or both assumptions were violated). For significant effects, post-hoc comparisons were performed using Tukey's HSD test for ANOVA results, or Dunn's test with Bonferroni correction for Kruskal-Wallis results, to identify specific differences between factor levels (species/maturity stage). Ontogenetic shifts in stable isotope values ($\delta^{13}C$ and $\delta^{15}N$) relative to standard length (SL) were investigated using segmented linear regression. This method, implemented with the segmented package in R (Muggeo, 2008), identified significant breakpoints where isotopic signatures changed with size, reflecting potential shifts in feeding strategies or habitat use. Analyses were conducted separately for each species and for each stable isotope. In this study, the results from SCA and SIA were not significantly different between the two sampling years, and consequently, the data were pooled into a single dataset for subsequent analyses. All analyses were conducted in R version 4.3.2, and results were considered significant at $\alpha = 0.05$.

## 3. Results

### 3.1. Length-weight relation and growth modelling

A total of 860 samples were collected and analysed to examine the relationships between standard length, body weight, and otolith dimensions. The length of *D. watasei* ranged from 60 mm to 165 mm, and body weight from 2.1 to 50.4 g, while *S. japonicus* specimens ranged from 85 to 178 mm, and from 6.1 to 108 g (Table 1). *Diaphus watasei* exhibited a near-isometric growth pattern, as indicated by the regression coefficient (b = 3.07), which did not significantly differ from the theoretical value of 3 (*t*-test, $p > 0.05$, df = 490). In contrast, *S. japonicus* showed a negative allometric growth pattern (b = 2.79), significantly lower than the isometric threshold (*t*-test, $p < 0.05$, df = 366).

A total of 290 and 380 otoliths from *D. watasei* and *S. japonicus* respectively have allowed for a clear reading of daily increments. Daily growth increments (age proxy) were obtained by summing up all the daily growth increments. Age estimated was ranged from 130 to 670 for *D. watasei* (355.9 ± 65.7 and 517.5 ± 91.8, respectively for the juvenile and adult life stage) and 190–640 for *S. japonicus* (227.5 ± 27.24 and 421.2 ± 107.8, respectively for the juvenile and adult life stage). Based on the observed data, the standard von Bertalanffy growth model provided a more accurate estimation of the growth parameters for both species (Supplementary Material S1). In *Diaphus watasei,* the estimated growth parameters were described by $L(t) = 237.94 \times (1 - e^{-0.0015(t+71.83)})$ and *S. japonicus* $L(t) = 232.66 \times (1 - e^{-0.0020(t+55.06)})$ (Supplementary material S1).

### 3.2. Diet preferences

A total of 5340 prey items belonging to 22 prey taxa were identified from 860 stomach samples. SCArevealed that both species exhibited a predominantly nektophagous feeding strategy, with diets largely composed of mesopelagic fishes. Teleosts constituted the predominant prey category for both juvenile and adult *Diaphus watasei* (% PSIRI=58.57 % and 50.06 %, respectively), with *Maurolicus muelleri* and *Myctophum spp.* being the most frequent taxa. Decapod crustaceans (25.95 % for juveniles; 13.39 % for adults) and euphausiids (15.47 % and 11.99 %, respectively) followed in importance. Cephalopods (8.52 %) were exclusively recorded in the adult diet. In juvenile *S. japonicus*, microbenthic organisms constituted the primary prey group (PSIRI = 53.32 %), followed by teleosts (22.57 %) and decapods

**Table 1**
Biological parameters (mean ± standard error) of *Diaphus watasei* and *Synagrops japonicus* for juvenile and adult life stages in the East China Sea, including coefficients 'a' and 'b' from the Length-Weight Relationship (LWR) equation ($W = aTL^b$). n: sample size; SL: Standard Length (mm); W: Total weight (g); Age: Age (days); OL: Otolith length (mm); OW: Otolith width (mm); a: intercept of the LWR equation; b: slope of the LWR equation (allometric coefficient). These descriptive statistics, along with the allometric coefficients, provide an overview of the sampled populations' growth characteristics and morphology.

| Parameters | | n | SL (mm) | W (g) | Age (days) | OL (mm) | Ow (mm) | a | b |
|---|---|---|---|---|---|---|---|---|---|
| *Diaphus watasei* | Juvenile | 113 | 109 ± 14.5 | 12.2 ± 3.3 | 355.9 ± 65.7 | 5.3 ± 0.8 | 3.5 ± 0.5 | 6.47 | 3.07 |
| | Adult | 274 | 137.8 ± 13.0 | 24.9 ± 8.0 | 517.5 ± 91.8 | 7.5 ± 1.0 | 4.5 ± 0.4 | | |
| *Synagrops japonicus* | Juvenile | 95 | 96.7 ± 14.5 | 10.5 ± 2.0 | 227.5 ± 27.24 | 4.1 ± 0.1 | 2.7 ± 0.08 | 3.11 | 2.79 |
| | Adult | 378 | 140.2 ± 18.6 | 33.2 ± 15.9 | 421.2 ± 107.8 | 5.4 ± 0.7 | 3.2 ± 0.2 | | |

(11.93 %). In contrast, adults' life stage diet was dominated by mesopelagic teleosts (57.03 %), decapod crustaceans (22.64 %), and euphausiids (12.36 %), with a minor contribution from cephalopods (5.21 %) (Table 2).

Principal Component Analysis (PCA) on major prey categories explained 89.86 % of the total variance, revealing clear functional segregation among groups (Fig. 2). The first axis (PC1, 75.99 %) drove a major habitat partitioning, isolating juvenile S. japonicus strongly correlated with Annelida and Mollusca from all other groups. The second axis (PC2, 13.87 %) differentiated the pelagic cluster based on prey size: juvenile *D. watasei* were associated with Copepoda, reflecting a zooplanktivorous strategy, whereas adults of both species converged closely around micronektonic prey vectors (Teleost, Decapoda, Cephalopod, and Euphausiacea).

### 3.3. Stable isotope compositions

Stable $\delta^{15}N$ isotope values showed significant differences among consumer groups (Kruskal–Wallis, $\delta^{15}N$, $\chi^2 = 51.30$, $p < 0.05$), with the exception between adult *S. japonicus* and juvenile *D. watasei* ($p > 0.05$), as well as between the juvenile stages of the two species ($p > 0.05$), according to Dunn's post hoc test with *D. watasei* displaying significant high mean values. Similarly, $\delta^{13}C$ isotope values varied significantly among consumer groups (Kruskal–Wallis, $\delta^{13}C$, $\chi^2 = 29.41$, $p < 0.05$), except between the adult stages of both species ($p > 0.05$) and between their respective juvenile stages ($p > 0.05$), as indicated by Dunn's post hoc comparisons. $\delta^{15}N$ values ranged from 8.83 ‰ to 14.26 ‰, with means of 10.97 ± 0.97 ‰ and 10.49 ± 0.68 ‰ in juvenile *D. watasei* and *S. japonicus*, respectively, and 12.39 ± 0.59 ‰ and 11.51 ± 0.73 ‰ in adults, and $\delta^{13}C$ values ranged from –20.19 ‰ to –17.29 ‰, with mean values of –19.49 ± 0.54 ‰ and –19.05 ± 0.14 ‰ in juveniles of *D. watasei* and *S. japonicus*, respectively, and –18.51 ± 0.46 ‰ and –18.69 ± 0.41 ‰ in adults (Table 3).

Segmented regression analysis revealed clear size-related shifts in the isotopic signatures of both species. In *S. japonicus*, a significant breakpoint was detected at 126.7 mm, beyond which the increase in $\delta^{15}N$ values with body size markedly slowed (slope decreasing from 0.050 to 0.006). A comparable pattern was observed in *D. watasei*, with a

**Table 2**
Composition of the diet of *Diaphus watasei* and *Synagrops japonicus* for juvenile and adult life stages by percentage of prey by wet weight (%PW), percentage of prey by number(%PN), frequency of occurrence (%FO), and percentage of the Prey-Specific Index of Relative Importance(%PSIRI).

| Prey groups | *Diaphus watasei* juvenile | | | | *Diaphus watasei* adult | | | | *Synagrops japonicus* juvenile | | | | *Synagrops japonicus* adult | | | |
|---|---|---|---|---|---|---|---|---|---|---|---|---|---|---|---|---|
| | %PW | %PN | %FO | % PSIRI | %PW | %PN | %FO | % PSIRI | %PW | %PN | %FO | % PSIRI | %PW | %PN | %FO | % PSIRI |
| Euphausiacea | | | | | | | | | | | | | | | | |
| *Euphausia nana* | | | | | 9.18 | 17.68 | 29.84 | 4.01 | | | | | 6.24 | 17.55 | 33.70 | 4.01 |
| *Pseudeuphausia* sp. | | | | | 9.89 | 17.50 | 27.23 | 3.73 | | | | | | | | |
| *Pseudeuphausia sinica* | | | | | | | | | | | | | 6.70 | 17.41 | 32.60 | 3.93 |
| *Euphausiacea* unidentified | 14.00 | 21.45 | 41.59 | 7.37 | 13.66 | 22.82 | 23.30 | 4.25 | 28.82 | 21.54 | 31.58 | 7.95 | 7.50 | 16.91 | 36.26 | 4.42 |
| Amphipoda unidentified | 0.48 | 22.23 | 36.28 | 4.12 | 1.24 | 22.38 | 32.20 | 3.80 | 1.59 | 20.68 | 37.89 | 4.22 | 0.32 | 22.12 | 24.54 | 2.75 |
| *Polychaeta* unidentified | | | | | | | | | 5.89 | 26.88 | 56.84 | 9.31 | | | | |
| *Scaphopoda* unidentified | | | | | | | | | 5.39 | 31.24 | 82.11 | 15.04 | | | | |
| *Gastropoda* unidentified | | | | | | | | | 40.54 | 33.85 | 77.89 | 28.97 | | | | |
| *Copepoda* unidentified | 0.04 | 22.46 | 35.40 | 3.98 | 1.25 | 24.15 | 21.73 | 2.76 | | | | | | | | |
| Decapoda | | | | | | | | | | | | | | | | |
| *Heterocaspus* sp. | 19.08 | 19.74 | 45.13 | 8.76 | 14.69 | 16.86 | 46.60 | 7.35 | | | | | 11.14 | 15.50 | 28.21 | 3.76 |
| *Plesionika* sp. | 23.21 | 26.00 | 23.01 | 5.66 | 18.51 | 21.20 | 25.39 | 5.04 | | | | | 13.63 | 15.88 | 22.34 | 3.30 |
| *Oplophorus* sp. | 32.08 | 27.16 | 16.81 | 4.98 | 23.54 | 22.52 | 18.85 | 4.34 | | | | | 15.49 | 16.91 | 45.42 | 7.36 |
| *Systellaspis* sp. | | | | | | | | | | | | | 13.04 | 16.64 | 23.08 | 3.42 |
| Decapoda unidentified | 21.43 | 26.33 | 27.43 | 6.55 | 17.73 | 22.38 | 26.70 | 5.36 | 37.48 | 22.19 | 40 | 11.93 | 13.46 | 19.32 | 29.30 | 4.80 |
| Teleostei | | | | | | | | | | | | | | | | |
| *Diaphus* sp. | 37.29 | 25.39 | 16.81 | 5.27 | 33.17 | 20.79 | 18.32 | 4.94 | | | | | 28.33 | 20.55 | 30.77 | 7.52 |
| *Myctophum* sp. | 40.81 | 27.34 | 42.48 | 14.48 | 36.63 | 24.97 | 43.46 | 13.39 | | | | | 26.61 | 20.52 | 14.29 | 3.37 |
| *Maurolicus muelleri* | 38.29 | 27.22 | 61.06 | 20.00 | 27.38 | 22.48 | 64.40 | 16.05 | | | | | 23.24 | 23.53 | 45.89 | 10.96 |
| *Benthosema fibulatum* | 37.27 | 28.19 | 30.09 | 9.85 | 28.21 | 21.97 | 33.25 | 8.51 | | | | | 22.55 | 18.10 | 27.11 | 5.51 |
| *Argyropelecus* sp. | | | | | | | | | | | | | 25.10 | 18.32 | 45.05 | 9.78 |
| *Polyipnus* sp. | | | | | | | | | | | | | 19.68 | 14.95 | 26.01 | 4.50 |
| Teleost unidentified | 39.79 | 27.86 | 26.55 | 8.98 | 32.49 | 21.18 | 26.70 | 7.17 | 69.7 | 17.82 | 51.58 | 22.57 | 32.50 | 20.00 | 58.61 | 15.39 |
| *Cephalopoda* unidentified | | | | | 49.76 | 25.96 | 22.51 | 8.52 | | | | | 45.91 | 15.97 | 16.85 | 5.21 |

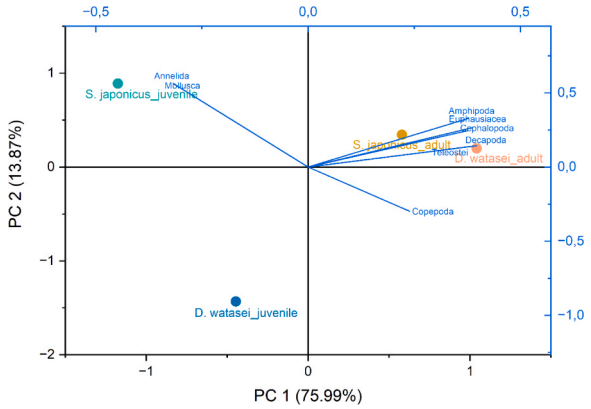


**Fig. 2.** Principal Component Analysis (PCA) biplot of major prey categories from *Diaphus watasei* and *Synagrops japonicus* across juvenile and adult stages. The plot illustrates the segregation of consumer groups (large colored dots) and the contribution of individual prey items (blue vectors) to the dietary differentiation. The first two principal components (PC1 and PC2 explain 75.99 % and 13.87 % of the total variance, respectively, totaling 89.86 %). PC1 primarily differentiates groups based on overall dietary composition, while PC2 highlights secondary gradients in prey utilization. This visualization clearly demonstrates the distinct dietary patterns and trophic partitioning among species and life stages.

**Table 3**
Mean values (± standard error) of stable isotopes (δ13 C and δ15 N, in ‰) and trophic position (TP) for *Diaphus watasei* and *Synagrops japonicus* in the East China Sea, stratified by life stage. n: sample size. These values characterize the average isotopic signatures and trophic levels of each group.

| Species | Life stage | n | $\delta^{15}$N (‰) | $\delta^{1}$ $^{3}$C (‰) | TP |
|---|---|---|---|---|---|
| *D. watasei* | Juvenile | 23 | 10.97 ± 0.97 | -19.49 ± 0.54 | 2.95 ± 0.08 |
| | Adult | 26 | 12.39 ± 0.59 | -18.51 ± 0.46 | 3.37 ± 0.03 |
| *S. japonicus* | Juvenile | 21 | 10.49 ± 0.68 | -19.05 ± 0.14 | 2.81 ± 0.07 |
| | Adult | 27 | 11.51 ± 0.73 | -18.69 ± 0.41 | 3.11 ± 0.03 |

breakpoint at 117.4 mm indicating a similar reduction in the rate of $\delta^{1}$ $^{5}$N enrichment (slope declining from 0.035 to 0.006) beyond this size. Analysis of $\delta^{1}$ $^{3}$C further highlighted species-specific ontogenetic dynamics: in *S. japonicus*, a breakpoint at 186.5 mm revealed a slight enrichment in $\delta^{1}$ $^{3}$C up to that size (slope = 0.009), followed by a significant depletion in larger individuals (slope = −0.016), whereas in *D. watasei*, a breakpoint at 116.3 mm indicated a slowdown in $\delta^{1}$ $^{3}$C enrichment with increasing body size (slope decreasing from 0.024 to 0.006)(Figs. 3 and 4, Supplementary material S2).

### 3.4. Niche estimation and overlap

Based on stomach content composition, revealed a high intraspecific trophic overlap based on Pianka's index between juvenile and adult life stages of *D. watasei* (0.98), indicating strong ontogenetic dietary similarity. In contrast, *S. japonicus* exhibited low intraspecific overlap (0.26), suggesting marked ontogenetic dietary segregation. Interspecific comparisons showed low trophic overlap between the juvenile stages of both species (0.19) and between juvenile *S. japonicus* and adult *D. watasei* (0.17). However, a substantial overlap was observed between adult *D. watasei* and adult *S. japonicus* (0.69). The standardized Levin's niche index (BSTA) indicated a relatively narrow niche breadth for all groups, except for adult S. japonicus, which displayed a comparatively broader trophic niche (Table 4). In isotopic space, the size of the isotopic niche (95 % credibility region) reveals distinct patterns. Juvenile *D. watasei* displayed the largest niche area (12.56 ± 3.63 ‰$^{2}$), indicating high inter-individual variability in assimilated food sources in isotopic space. In contrast, juvenile *S. japonicus* exhibited the smallest niche area (3.36 ± 1.17), supporting the hypothesis of trophic specialization at this life stage (Fig. 5).

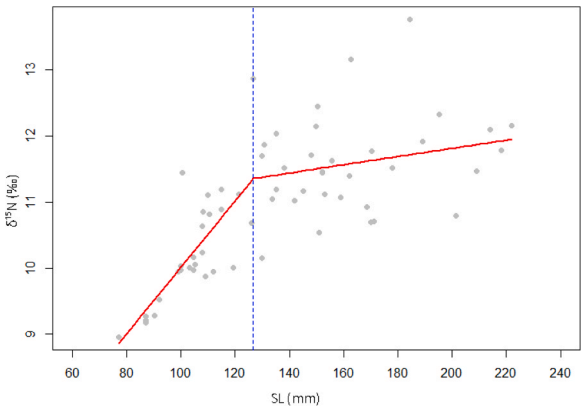


**Fig. 3.** Segmented regression analysis of $\delta^{1}$ $^{5}$N values against Standard Length (SL, mm) for *Synagrops japonicus*. The plot illustrates a significant breakpoint detected at approximately 126.7 mm, indicating a marked change in the ontogenetic trajectory of trophic position. Beyond this breakpoint, the increase in $\delta^{1}$ $^{5}$N values with body size significantly slows (initial slope = 0.050, post-breakpoint slope = 0.006). The grey points represent individual $\delta^{1}$ $^{5}$N values, and the red lines show the fitted segmented regression model with the vertical dashed line indicating the breakpoint.

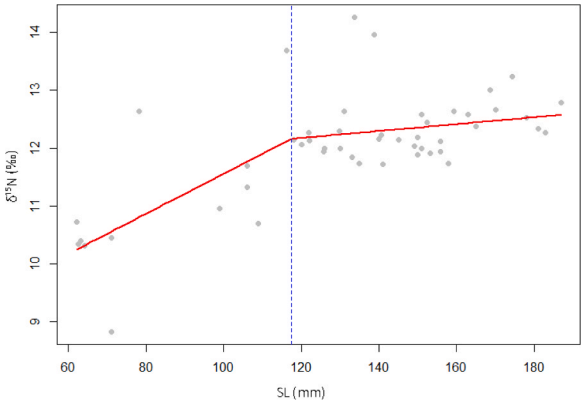


**Fig. 4.** Segmented regression analysis of $\delta^{1}$ $^{5}$N values against Standard Length (SL, mm) for *Diaphus watasei*. The plot illustrates a significant breakpoint detected at approximately 117.4 mm, indicating a marked change in the ontogenetic trajectory of trophic position. Beyond this breakpoint, the increase in $\delta^{1}$ $^{5}$N values with body size significantly slows (initial slope = 0.035, post-breakpoint slope = 0.006). The grey points represent individual $\delta^{1}$ $^{5}$N values, and the red lines show the fitted segmented regression model with the vertical dashed line indicating the breakpoint.

**Table 4**
Pianka's trophic niche overlap and standardized Levin's niche breadth values (BSTA) indices among species and ontogenetic stages for *Diaphus watasei* and *Synagrops japonicus* in the East China Sea. Adu: Adult stage; Juv: Juvenile stage. This table quantifies the extent of dietary resource sharing and specialization among the different consumer groups.

| Species | *D. watasei*_Juv | *D. watasei*_Adu | *S. japonicus*_Juv | *S. japonicus*_Adu |
|---|---|---|---|---|
| *D.watasei*_Juv | | 0.98 | 0.19 | 0.69 |
| *D.watasei*_Adu | | | 0.17 | 0.69 |
| *S.japonicus*_Juv | | | | 0.26 |
| **Levin niche ($B_{sta}$)** | 0.30 | 0.34 | 0.25 | 0.69 |
| **TPsca** | 3.96 | 3.99 | 3.42 | 3.88 |

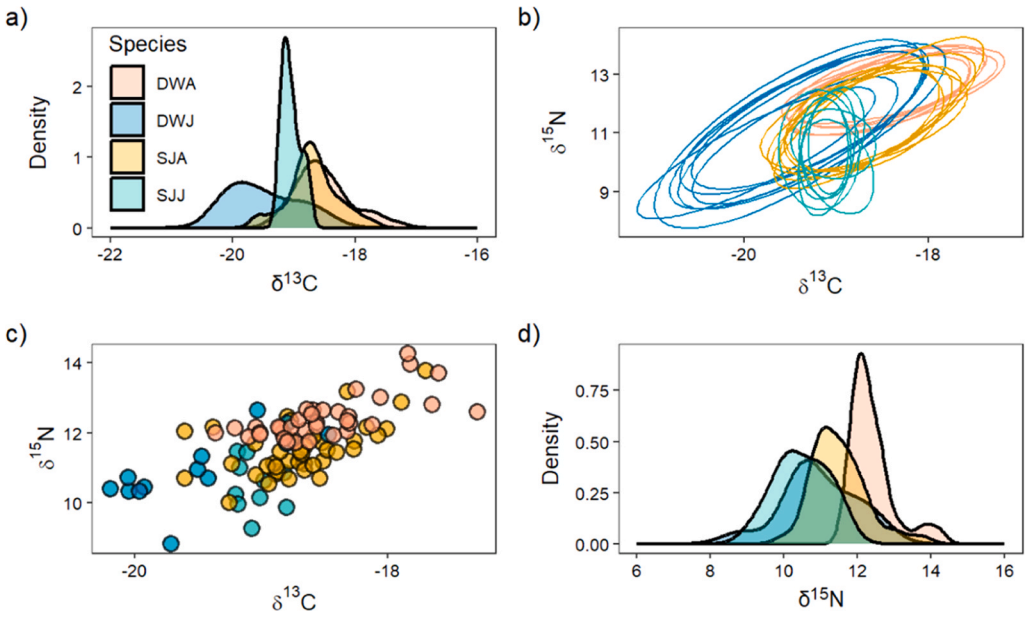


**Fig. 5.** Isotopic niche plots for *Diaphus watasei* (juvenile: blue-green, adult: light orange) and *Synagrops japonicus* (juvenile: light blue, adult: goldenrod). Panel (a) displays kernel density distributions of $\delta^{13}C$ values, illustrating resource utilization differences. Panel (b) shows Bayesian standard ellipses of the isotopic niche for each group (95 % credibility region), indicating dietary overlap and segregation in $\delta^{13}C$ and $\delta^{15}N$ space. Panel (c) presents a scatter plot of individual $\delta^{15}N$ versus $\delta^{13}C$ values, with points colored by species and life stage. Panel (d) displays kernel density distributions of $\delta^{15}N$ values, illustrating trophic position differences. DWA: *Diaphus watasei* Adult; DWJ: *Diaphus watasei* Juvenile; SJA: *Synagrops japonicus* Adult; SJJ: *Synagrops japonicus* Juvenile.

Isotopic niche regions ($N_R$) differed among the four consumer groups (Fig. 6). A substantial trophic overlap (83.15 %) was observed between adults of *D. watasei* and *S. japonicus*, whereas juveniles of *S. japonicus* showed minimal overlap (10.61 %) with adult *D. watasei*. Conversely, the very low overlap between adult *D. watasei* and juvenile *S. japonicus* further supports near-complete trophic segregation. A high degree of overlap (80.87 %) between juvenile and adult *S. japonicus* confirms strong ontogenetic continuity already highlighted by stomach content analysis.

## 4. Discussion

### 4.1. Discussion length weight relationship

Age estimation based on daily otolith increment counts proved to be a reliable and robust method for both species, *D. watasei* and *S. japonicus*, supported by the substantial number of otoliths examined (290 and 380, respectively). The observed age ranges (130–670 days for *D. watasei* and 190–640 days for *S. japonicus*) encompass a significant portion of their life cycle, enabling a detailed analysis of their ontogenetic development. The distinct mean ages identified for the juvenile and adult stages of each species confirm the presence of well-defined life phases and support the ontogenetic framework adopted.

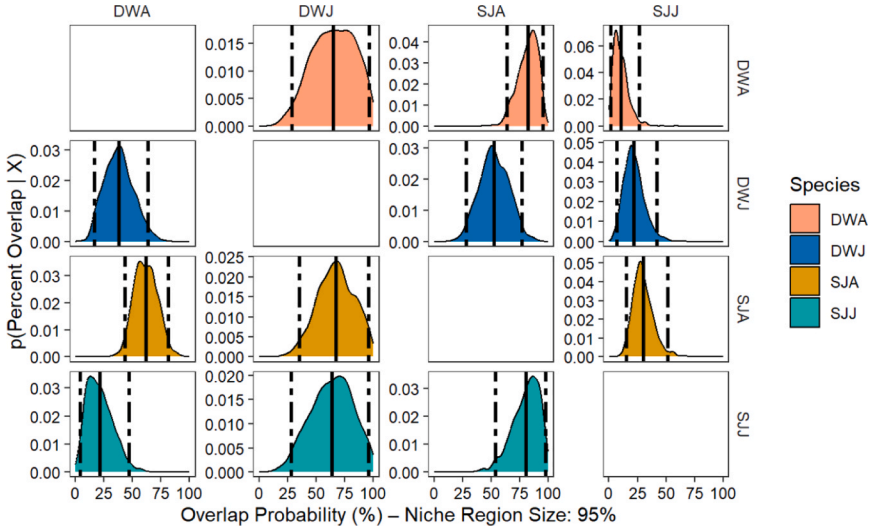


**Fig. 6.** Bayesian analysis of isotopic niche overlap (NicheROVER results) for *Diaphus watasei* and *Synagrops japonicus* across juvenile and adult stages. The plot shows the posterior probability (%) for an individual from the consumer group in the row to occupy the 95 % isotopic niche region of the consumer group in the column. Posterior means are displayed as bold lines, and 95 % credible intervals as dashed lines. Grouping and color codes (DWA, DWJ, SJA, SJJ) correspond to those in Fig. 5. This figure quantifies the extent of isotopic niche overlap and segregation among species and life stages.

In this study, *Synagrops japonicus* exhibited negative allometric growth, consistent with a previous study in the Arabian Sea and in the southwest coast of India reporting a similar length–weight pattern for the species (Renjith et al., 2020; Augustine et al., 2022). This type of growth can be considered a way of balancing energy use (Battaglia et al., 2015; Mcbride et al., 2015), where, upon reaching a certain body size, potentially corresponding to sexual maturity, acquired energy is preferentially allocated to reproductive output rather than somatic growth. This shift could potentially provide an adaptive advantage in mesopelagic environments, particularly for species engaged in active vertical migrations (Moku et al., 2000). Negative allometry has also been reported in several other mesopelagic fishes, including non-migratory species such as *Ichthyococcus ovatus* (Phosichthyidae), *Sternoptyx diaphana* (Sternoptychidae), *Diretmus argenteus* and *Diretmoides paucir-adiatus* (Diretmidae), *Zaphotias pedaliotus* (Stomiidae), and *Electrona risso* (Myctophidae), as well as in migratory myctophids like *Diaphus dumerilii* and *Diaphus perspicillatus* (Czudaj et al., 2022).

In contrast, *Diaphus watasei* exhibited nearly isometric growth, a pattern typical of many lanternfish species (Badouvas et al., 2022; Czudaj et al., 2022), where the body mass increases proportionally with length. This result is consistent with other regional studies on myctophids, although considerable variation has been reported often attributed to local environmental conditions, prey availability, or sexual maturation stage (Vipin et al., 2011; López-Pérez et al., 2020). In the East China Sea, Zhang and Guo (2024) previously reported allometric growth in *D. watasei*, a finding that contrasts with the present results. However, this discrepancy may be explained by differences in size range between the sampled populations; our dataset included marginal size classes (60–165 mm), which were not considered in their study. This methodological variation is significant and highlights a persistent problem in myctophid research. The inclusion of extreme size classes particularly small juveniles (<80 mm) and large adults (>150 mm) can significantly affect the parameters of length–weight relationships. Growth patterns in *D. watasei* may vary markedly across ontogenetic stages, with juvenile individuals exhibiting a tendency toward negative allometry. The inclusion of these marginal sizes in our dataset may therefore explain the reversion toward isometric growth observed in our analysis.

### 4.2. Ontogenetic trophic shift

The dietary composition of mesopelagic fishes in the ECS is poorly documented; however, the species analysed in this study demonstrated significant variability in feeding strategies, with distinct species-specific patterns supported by our multi-tracer methodology. While stomach content analysis revealed a shift toward larger prey such as cephalopods in adulthood, stable isotope analysis provided quantitative evidence of this trophic elevation. Most studies report that mesopelagic fishes predominantly feed on copepods and various crustaceans (Tanaka et al., 2013; Badouvas et al., 2024). This general pattern contrasts with our findings, in which both species displayed ontogenetic shifts characterised by distinct dietary preferences between life stages.

For *Diaphus watasei*, the diet was found to be relatively balanced, consisting of mesopelagic fish, crustaceans, and, to a lesser extent, copepods. The discrepancy likely results from the broader size range examined in the present study (60–165 mm) and the use of the PSIRI method, which reduces overestimation of rare but voluminous prey (Brown et al., 2012). The species displayed a narrow dietary spectrum but a marked ontogenetic shift, quantitatively supported by segmented regression analysis (Fig. 4). The significant $\delta^{15}N$ breakpoint at 117.4 mm corresponds to the transition to a more piscivorous and cephalopod-based diet, reflecting an increase in trophic position. $\delta^{13}C$ values stabilized beyond 116.3 mm, suggesting that adults occupy a consistent habitat, likely reducing vertical migration amplitude compared to juveniles (Gartner et al., 1997; Yamada et al., 2007; Sassa et al., 2016). These results indicate that adult feeding habits may reflect the exploitation of relatively homogeneous habitats with stable prey availability, a major adaptive advantage in the variable mesopelagic zone (Suntsov and Brodeur, 2008; Timmerman et al., 2021).

A clear ontogenetic shift was observed in *S. japonicus*, transitioning from a benthic-oriented juvenile phase to a more benthopelagic adult foraging behavior. Juveniles fed predominantly on macrobenthic prey, particularly benthic invertebrates (Gastropoda, Scaphopoda) and small polychaetes. This reliance on sedentary prey is characteristic of demersal species constrained by limited locomotory capacity and reduced gape size, promoting energy-efficient foraging within nursery habitats (Scharf et al., 2000; Fanelli and Cartes, 2010). Such ontogenetic niche conservatism aligns with ecological theory, which predicts that juveniles reduce intraspecific competition by exploiting a narrower prey spectrum (Labropoulou and Eleftheriou, 1997), as reflected in the low Levin's niche breadth estimated for juveniles (Table 4).

Adults exhibited a marked expansion of their trophic niche and position, as demonstrated by the broader Levin's index and the increase in $\delta^{15}N$ values up to the 126.7 mm breakpoint (Fig. 3; Table 2). This transition involved active benthopelagic foraging, targeting vertically migrating prey such as myctophids, pelagic crustaceans, euphausiids, and cephalopods. Capturing this more evasive prey requires enhanced swimming performance (Scharf et al., 2000). $\delta^{13}C$ depletion observed in large adults (>186.5 mm) supports a functional decoupling from the benthic food web in favour of pelagic carbon sources (Supplementary material S2). The inclusion of diverse, higher-trophic-level prey underscores the ontogenetic trophic shift typical of deep-sea generalists and highlights the role of diel vertical migrators in transferring energy to demersal predators (Drazen and Sutton, 2017; Afonso et al., 2014).

### 4.3. Trophic niche expansion and overlap

The interspecific differentiation in diet between *D. watasei* and *S. japonicus* reveals contrasting ecological strategies facilitating coexistence within the same habitat. Juveniles of both species exhibited low dietary overlap (Pianka's index = 0.19), indicating clear resource partitioning driven by the spatial segregation described in Section 4.2: *S. japonicus* juveniles are strictly demersal foragers, while *D. watasei* rely on vertically migrating pelagic sources.

In contrast, adult stages showed considerable convergence in their diet (Pianka's index = 0.69). This increased overlap is a direct consequence of the ontogenetic niche expansion observed in S. japonicus, which transitions to benthopelagic foraging in adulthood. Despite this convergence, adult S. japonicus maintained a broader trophic niche width compared to *D. watasei* (Table 4), reflecting a more generalist strategy. This pattern aligns with the theory of competitive coexistence, where interspecific competition is mitigated through partial niche divergence (Eurich et al., 2018; Luo et al., 2024). Similar dietary segregation strategies between vertically migrating *Myctophidae* and non-migratory taxa have been documented to facilitate the coexistence of dominant mesopelagic groups (Bernal et al., 2023).

The convergence in adult trophic structure appears to result from asymmetrical trophic dependence rather than simple resource competition: *S. japonicus* incorporates *D. watasei* as a key prey item (Hopkins and Sutton, 1998; Sutton et al., 2008). This predator-prey interaction explains the apparent discrepancy between the high dietary overlap and the persistent isotopic differences. While diets converge, vertical habitat segregation likely remains influential. The consistently higher $\delta^{15}N$ values in juvenile *S. japonicus* compared to juvenile *D. watasei* despite both occupying mid-trophic positions reflects the enrichment of basal particulate organic matter (POM) with depth, differentiating the demersal resident (*S. japonicus*) from the vertical migrator (*D. watasei*) (McClain-Count et al., 2017; Choy et al., 2015).

Regional comparisons suggest that these isotopic variations must be interpreted in the context of local baselines. Absolute $\delta^{15}N$ values in our study were slightly higher than those reported for myctophids in the Southern Ocean (Saunders et al., 2019) or the subtropical North Pacific

(Choy et al., 2015), likely reflecting regional variations in isotopic baselines rather than true differences in trophic position (Magozzi et al., 2017). Similarly, the $\delta^{1}$ $^{3}$C variations we observed (–18.51 to –19.49 ‰) corroborate findings from other ECS studies (Asante et al., 2008; Chen et al., 2025), confirming that while trophic niches overlap in adulthood, the two species maintain subtle but ecologically meaningful differences in primary carbon source reliance. Overall, coexistence is maintained through a combination of ontogenetic spatial segregation in juveniles and asymmetrical trophic interaction in adults.

## 5. Conclusion

This study enhances our understanding of the mechanisms structuring mesopelagic communities and underscores the crucial role of ontogenetic differentiation in maintaining marine biodiversity. The coexistence of *Diaphus watasei* and *S. japonicus* relies on a delicate relationship between spatial segregation in juveniles and trophic convergence in adults. Our isotopic and stomach content analyses reveal that this adult convergence does not stem from simple competition but rather from an asymmetric trophic relationship in which *S. japonicus* incorporates *D. watasei* into its diet, illustrating niche expansion rather than displacement. This trophic plasticity, characterized by size-related dietary shifts (isotopic breakpoints), suggests a certain resilience in these species. However, the strong dependence of juveniles on benthic networks and of adults on vertical migrators highlights their potential vulnerability to disturbances affecting the biological pump and the structure of zooplankton communities. In the context of climate change and increasing pressure from deep-sea fisheries, understanding these benthopelagic couplings is essential for predicting the response of continental slope ecosystems.

## Declaration of Competing Interest

The authors declare that they have no known competing financial interests or personal relationships that could have appeared to influence the work reported in this paper.

## Acknowledgments

This work was supported by the National Natural Science Foundation of China (#42276092) and the Program for Professor of Special Appointment (Eastern Scholar) at Shanghai Institutions of Higher Learning. The authors thank the staff at "*Zheling Fishery 74016* " for their assistance with sample collection and preparation.

### *Author Contributions*

Ngo Nola Mara Dorine and Yunlai Li conceived and designed the experiments. Ngo Nola Mara Dorine performed the experiments and analyzed the data with the help of Mboglen, Luhao Fan and YL. Ngo Nola Mara Dorine wrote the manuscript with the advice of Mboglen David and Yunkai Li. All authors provided editorial feedback and agreed that the manuscript should be submitted in this form.

## Appendix A. Supporting information

Supplementary data associated with this article can be found in the online version at doi:10.1016/j.rsma.2025.104743.

## Data availability

Data will be made available on request.

## References

Afonso, P., McGinty, N., Graça, G., Fontes, J., Inácio, M., Totland, A., Menezes, G., 2014. Vertical migrations of a deep-sea fish and their role in trophic dynamics. Deep-Sea Res. I 83, 22–34.

Alonso, M.K., Crespo, E.A., Aníbal García, N., Noemí Pedraza, S., Mariotti, P.A., Mora, N. J., 2002. Fishery and ontogenetic driven changes in the diet of the spiny dogfish, *Squalus acanthias*, in Patagonian waters, Argentina. Environ. Biol. Fishes 63, 193–202. https://doi.org/10.1023/A:1014229432375.

Asante, K.A., Agusa, T., Mochizuki, H., Ramu, K., Inoue, S., Kubodera, T., Takahashi, S., Subramanian, A., Tanabe, S., 2008. Trace elements and stable isotopes (δ13C and δ15N) in shallow and deep-water organisms from the East China Sea. Environ. Pollut. 156, 862–873. https://doi.org/10.1016/j.envpol.2008.05.020.

Augustine, S., Lika, K., Kooijman, S.A.L.M., 2022. The comparative energetics of the chondrichthyans reveals universal links between respiration, reproduction and lifespan. J. Sea Res. 185, 102228. https://doi.org/10.1016/J.SEARES.2022.102228.

Badouvas, N., Somarakis, S., Tsagarakis, K., 2022. Length–weight relations of 16 mesopelagic fishes (Actinopterygii: myctophiformes and stomiiformes) from the eastern Mediterranean Sea. Acta Ichthyol. Piscat. 52, 279–283. https://doi.org/10.3897/aiep.52.97577.

Badouvas, N., Tsagarakis, K., Somarakis, S., Karachle, P.K., 2024. Feeding habits and prey composition of six mesopelagic fish species from an Isolated Central Mediterranean basin. Fishes 9 (7). https://doi.org/10.3390/fishes9070277.

Battaglia, P., Malara, D., Ammendolia, G., Romeo, T., Andaloro, F., 2015. Relationships between otolith size and fish length in some mesopelagic teleosts (myctophidae, paralepididae, phosichthyidae and stomiidae). J. Fish. Biol. 87 (3), 774–782. https://doi.org/10.1111/jfb.12744.

Bensch, A., Gianni, M., Gréboval, D., Sanders, J.S., Hjort, A., 2009. Worldwide review of bottom fisheries in the high seas. Rev. 1 FAO Fisheries and Aquaculture Technical Paper No. 522. FAO, Rome, p. 145. Rev. 1.

Bernal, A., Tuset, V.M., Olivar, M.P., 2023. Multiple approaches to the trophic role of mesopelagic fish around the iberian peninsula. Animals 13 (5). https://doi.org/10.3390/ani13050886.

Brown, S.C., Bizzarro, J.J., Cailliet, G.M., Ebert, D.A., 2012. Breaking with tradition: redefining measures for diet description with a case study of the Aleutian skate *Bathyraja aleutica* (Gilbert 1896). Environ. Biol. Fishes 95 (1), 3–20. https://doi.org/10.1007/s10641-011-9959-z.

Cailliet, G.M., Smith, W.D., Mollet, H.F., Goldman, K.J., 2006. Age and growth studies of chondrichthyan fishes: the need for consistency in terminology, verification, validation, and growth function fitting. Environ. Biol. Fishes 77, 211–228. https://doi.org/10.1007/s10641-006-9105-5.

Campana, S.E., Jones, C.M., 1992. Analysis of otolith microstructure data. Can. Spec. Publ. Fish. Aquat. Sci. No. 117, 73–100.

Catul, V., Gauns, M., Karuppasamy, P.K., 2011. A review on mesopelagic fishes belonging to family Myctophidae. Rev. Fish. Biol. Fish. 21 (3), 339–354. https://doi.org/10.1007/s11160-010-9176-4.

Chen, X., Li, Z., Mboglen, D., Li, Y., 2025. Trophic partitioning and mercury accumulation in deep-sea fishes of the East China Sea. DeepSea Res. Part I Oceanogr. Res. Pap. 218. https://doi.org/10.1016/j.dsr.2025.104473.

Cheng, J., Cheung, W.W.L., Pitcher, T.J., 2009. Mass-balance ecosystem model of the East China Sea. Prog. Nat. Sci. 19 (10), 1271–1280. https://doi.org/10.1016/j.pnsc.2009.03.

Choy, C.A., Popp, B.N., Hannides, C.C.S., Drazen, J.C., 2015. Trophic structure and food resources of epipelagic and mesopelagic fishes in the north pacific subtropical Gyre ecosystem inferred from nitrogen isotopic compositions. Limnol. Oceano 60 (4), 1156–1171. https://doi.org/10.1002/lno.10085.

Czudaj, S., Möllmann, C., Fock, H.O., 2022. Length–weight relationships of 55 mesopelagic fishes from the eastern tropical North Atlantic: across- and within-species variation (body shape, growth stanza, condition factor). J. Fish. Biol. 101 (1), 26–41. https://doi.org/10.1111/jfb.15068.

Drazen, J.C., Sutton, T.T., 2017. Dining in the deep: the feeding ecology of deep-sea fishes (Annual Reviews Inc). Annu. Rev. Mar. Sci. 9 (1), 337–366. https://doi.org/10.1146/annurev-marine-010816-060543.

Eduardo, L.N., Lucena-Frédou, F., Mincarone, M.M., Soares, A., Le Loc'h, F., Frédou, T., Ménard, F., Bertrand, A., 2020. Trophic ecology, habitat, and migratory behaviour of the viperfish *Chauliodus sloani* reveal a key mesopelagic player. Sci. Rep. 10 (1). https://doi.org/10.1038/s41598-020-77222-8.

Eduardo, L.N., Mincarone, M.M., Sutton, T., Bertrand, A., 2024. Deep-pelagic fishes are anything but similar: a global synthesis. Ecol. Lett. 27 (9). https://doi.org/10.1111/ele.14510.

Eurich, J.G., McCormick, M.I., Jones, G.P., 2018. Direct and indirect effects of interspecific competition in a highly partitioned guild of reef fishes. Ecosph 9 (8). https://doi.org/10.1002/ecs2.2389.

Fanelli, E., Cartes, J.E., 2010. Temporal variations in the feeding habits and trophic levels of three deep-sea demersal fishes from the western Mediterranean Sea, based on stomach contents and stable isotope analyses. Mar. Ecol. Prog. Ser. 402, 213–232. https://doi.org/10.3354/meps08421.

FAO, 2014. The state of world fisheries and aquaculture 2014. FAO, Rome.

Gagliano, M., McCormick, M.I., Meekan, M.G., 2007. Survival against the odds: ontogenetic changes in selective pressure mediate growth-mortality trade-offs in a marine fish. Proc. R. Soc. B Biol. Sci. 274 (1618), 1575–1582.

Gartner Jr, J.V., Crabtree, R.E., Sulak, K.J., 1997. Feeding at depth. In: David, J.R., Grimaldo, E., Grimsmo, L., Alvarez, P., Herrmann, B., Tveit, G.M., Tiller, R., Slizyte, R., Aldanondo, N., Guldberg, T., Toldnes, B., Carvajal, A., Schei, M., Selnes, M., 2020. Investigating the potential for a commercial fishery in the Northeast Atlantic

utilizing mesopelagic species. ICES J. Mar. Sci. 77 (7–8), 2541–2556. https://doi.org/10.1093/icesjms/fsaa114.
Grossman, S.J., Hart, O.D., 1986. The costs and benefits of ownership: a theory of vertical and lateral integration. J. Polit. Econ. 94 (4), 691–719. https://doi.org/10.1086/261404.
Hopkins, T.L., Sutton, T.T., 1998. Midwater fishes and shrimps as competitors and resource partitioning in low latitude oligotrophic ecosystems. Mar. Ecol. Prog. Ser. 164, 37–45.
Hyslop, E.J., 1980. Stomach contents analysis-a review of methods and their application. J. Fish. Biol. 17, 411–429. https://doi.org/10.1111/j.1095-8649.1980.tb02775.x.
Iglesias, I.S., Santora, J.A., Fiechter, J., Field, J.C., 2023. Mesopelagic fishes are important prey for a diversity of predators. Front. Mar. Sci. 10. https://doi.org/10.3389/fmars.2023.1220088.
Kourantidou, M., Jin, D., 2022. Mesopelagic–epipelagic fish nexus in viability and feasibility of commercial-scale mesopelagic fisheries. Nat. Resour. Model. 35 (4). https://doi.org/10.1111/nrm.12350.
Krebs, C. J. (1999). Ecological Methodology. 2nd edition. Benjamin/Cummings, Menlo Park, California.
Labropoulou, M., Eleftheriou, A., 1997. The foraging ecology of two pairs of congeneric demersal fish species: importance of morphological characteristics in prey selection. J. Fish. Biol. 50, 324–340. https://doi.org/10.1111/j.1095-8649.1997.tb01361.x.
Le Cren, E.D., 1951. The length–weight relationship and seasonal cycle in gonad weight and condition in the perch (*Perca fluviatilis*). J. Anim. Ecol. 20 (2), 201–219.
Li, Y., Zhang, Y., 2012. Fisheries impact on the East China Sea shelf ecosystem for 1969-2000. Helgol. Mar. Res. 66 (3), 371–383. https://doi.org/10.1007/s10152-011-0278-8.
Li, Y., Zhang, Y., Hussey, N.E., Dai, X., 2016. Urea and lipid extraction treatment effects on δ15N and δ13C values in fish tissues. J. Fish Biol. 89, 312–321. https://doi.org/10.1111/jfb.12954.
Liang, C., Pauly, D., 2017. Fisheries impact on China's coastal ecosystems: unmasking a pervasive 'fishing down' effect. PLoS One 12 (6), e0179276.
Lombarte, A., Cruz, A., 2007. Otolith size trends in marine fish communities from different depth strata. J. Fish. Biol. 71 (1), 53–68.
López-Pérez, C., Olivar, M.P., Hulley, P.A., Tuset, V.M., 2020. Length–weight relationships of mesopelagic fishes from the equatorial and tropical AtlSLantic waters: influence of environment and body shape. J. Fish. Biol. 96 (6), 1388–1398. https://doi.org/10.1111/jfb.14307.
Luo, K., Yang, X., Zhou, Y., Yi, X., Zhao, C., Wang, J., He, X., Yan, Y., 2024. The sympatric coexistence mechanism: a case study of two penahia species in the Beibu Gulf, South China Sea. Anim 14 (6). https://doi.org/10.3390/ani14060849.
Magozzi, S., Yool, A., Vander Zanden, H.B., Wunder, M.B., Trueman, C.N., 2017. Using ocean models to predict spatial and temporal variation in marine carbon isotopes. Ecosphere 8 (5). https://doi.org/10.1002/ecs2.1763.
Mcbride, R.S., Somarakis, S., Fitzhugh, G.R., Albert, A., Yaragina, N.A., Wuenschel, M.J., Alonso-Fernández, A., Basilone, G., 2015. Energy acquisition and allocation to egg production in relation to fish reproductive strategies. Fish Fish 16 (1), 23–57. https://doi.org/10.1111/faf.12043.
McClain-Counts, J.P., Demopoulos, A.W.J., Ross, S.W., 2017. Trophic structure of mesopelagic fishes in the Gulf of Mexico revealed by gut content and stable isotope analyses. Mar. Ecol. 38, e12449. https://doi.org/10.1111/maec.12449.
Moku, M., Kawaguchi, K., Watanabe, H., Ohno, A., 2000. Feeding habits of three dominant myctophid fishes, Diaphus theta, Stenobrachius leucopsarus and S. nannochir, in the subarctic and transitional waters of the western North Pacific. Mar. Ecol. Prog. Ser. 207, 129–140. https://doi.org/10.3354/meps207129.
Morato, T., Watson, R., Pitcher, T.J., Pauly, D., 2006. Fishing down the deep. Fish Fish 7, 24–34. https://doi.org/10.1111/j.1467-2979.2006.00205.x.
Muggeo, V.M.R., 2008. Segmented: an R package to fit regression models with broken-line relationships. R. N. 8 (1), 20–25.
Ohshimo, S., Yasuda, T., Tanaka, H., Sassa, C., 2012. Biomass fluctuation of two dominant lanternfish Diaphus garmani and D. chrysorhynchus with environmental changes in the East China Sea. Fish. Sci. 78 (1), 33–39. https://doi.org/10.1007/s12562-011-0424-x.
Ozawa, T., Zinno, H., 1990. Studies on the bottom fishes of continental slope off Makurazaki, Southern Japan. Bull. Jpn. Soc. Fish. Oceano 54, 255–270.
Pauly, D., Piroddi, C., Hood, L., Bailly, N., Chu, E., Lam, V., Pakhomov, E.A., Pshenichnov, L.K., Radchenko, V.I., Palomares, M.L.D., 2021. The biology of mesopelagic fishes and their catches (1950– 2018) by commercial and experimental fisheries. J. Mar. Sci. Eng. 9 (10). https://doi.org/10.3390/jmse9101057.
Pianka, E.R., 1973. The structure of lizard communities further. Annu. Rev. Ecol. Evol. Syst. 4, 53–74.
Polis, G.A., Myers, C.A., Holt, R.D., 1989. The ecology and evolution of intraguild predation: potential competitors that eat each other. Annu. Rev. Ecol. Syst. 20 (1), 297–330.
Prellezo, R., Corrales, X., Andonegi, E., Bald, C., Fernandes-Salvador, J.A., Iñarra, B., Irigoien, X., Martin, A., Murillas-Maza, A., Tasdemir, D., 2024. Economic trade-offs of harvesting the ocean twilight zone: an ecosystem services approach. Ecosyst. Serv. 67. https://doi.org/10.1016/j.ecoser.2024.101633.
Quang, R.G.T., Kourantidou, M., Jin, D., 2024. Assessing the potential economic effects of mesopelagic fisheries as a novel source of fishmeal. Nat. Resour. Model. 37 (3). https://doi.org/10.1111/nrm.12398.
Rayegani, Anita, 2024. Mesopelagic mysteries: regulating an emerging resource amid uncertainty. Ocean Dev. Int. Law 55 (1–2), 1–24. https://doi.org/10.1080/00908320.2024.2313744.
Relini, G., 2015. MEDITS Handbook. Version n. 7. International bottom trawl survey in the Mediterranean. FAO–GFCM.
Renjith, R.K., Jha, P.N., Chinnadurai, S., Michael, B., Remesan, M.P., 2020. Length weight relationship of five deep sea fishes from Kerala, south west coast of India. J. Appl. Ichthyol. 36 (2), 259–260. https://doi.org/10.1111/jai.14015.
Ross, S.T., 1986. Resource partitioning in fish assemblages: a review of field studies. Copeia (2), 352–388.
Sassa, C., Tanaka, H., Ohshimo, S., 2016. Comparative reproductive biology of three dominant myctophids of the genus Diaphus on the slope region of the East China Sea. DeepSea Res. Part I Oceanogr. Res. Pap. 115, 145–158. https://doi.org/10.1016/j.dsr.2016.06.005.
Sassa, C., Tsukamoto, Y., Yamamoto, K., Tokimura, M., 2010. Spatio-temporal distribution and biomass of *Benthosema pterotum* (Pisces: Myctophidae) in the shelf region of the East China Sea. Mar. Ecol. Prog. Ser. 407, 227–241.
Saunders, R.A., Hill, S.L., Tarling, G.A., Murphy, E.J., 2019. Myctophid Fish (Family Myctophidae) are central consumers in the food web of the Scotia Sea (Southern Ocean). Front. Mar. Sci. 6. https://doi.org/10.3389/fmars.2019.00530.
Scharf, F.S., Juanes, F., Rountree, R.A., 2000. Predator size - prey size relationships of marine fish predators: interspecific variation and effects of ontogeny and body size on trophic-niche breadth. Mar. Ecol. Prog. Ser. 208, 229–248.
Serena, F., Mancusi, C., Marsili, L., Voliani, A., Neri, A., 2022. On the presence of Synagrops japonicus (acropomatiformes: synagropidae) in the Mediterranean Sea. ACTA ADRIAT 63 (1), 83–92.
Sharma, R., Barange, M., Agostini, V., Barros, P., Gutierrez, N.L., Vasconcellos, M., Fernandez Reguera, D., Tiffay, C., Levontin, P., 2025. Review of the state of world marine fishery resources – 2025 (eds). FAO Fisheries and Aquaculture Technical Paper, No. 721. FAO, Rome. https://doi.org/10.4060/cd5538en.
Shen, J., Cheng, Y., 1989. On the deep sea demersal fish communities of the East China Sea. Chin. J. Oceanol. Limnol. 7 (2), 159–168.
Sogard, S.M., 1997. Size-selective mortality in the juvenile stage of teleost fishes: a review. Bull. Mar. Sci. 60 (3), 1129–1157.
Suntsov, A.V., Brodeur, R.D., 2008. Trophic ecology of three dominant myctophid species in the northern California Current region. Mar. Ecol. Prog. Ser. 373, 81–96. https://doi.org/10.3354/meps07678.
Sutton, T.T., Porteiro, F.M., Heino, M., Byrkjedal, I., Langhelle, G., Anderson, C.I.H., Horne, J., Søiland, H., Falkenhaug, T., Godø, O.R., Bergstad, O.A., 2008. Vertical structure, biomass and topographic association of deep-pelagic fishes in relation to a mid-ocean ridge system. DeepSea Res. Part II Top. Stud. Oceanogr. 55 (1–2), 161–184. https://doi.org/10.1016/j.dsr2.2007.09.013.
Swanson, H.K., Lysy, M., Power, M., Stasko, A.D., Johnson, J.D., Reist, J.D., 2015. A new probabilistic method for quantifying n-dimensional ecological niches and niche overlap. Ecol 96. https://doi.org/10.1890/14-0235.1.
Szuwalski, C.S., Burgess, M.G., Costello, C., Gaines, S.D., 2017. High fishery catches through trophic cascades in China. Proc. Natl. Acad. Sci. 114 (4), 981–986.
Tanaka, H., Sassa, C., Ohshimo, S., Aoki, I., 2013. Feeding ecology of two lanternfishes *Diaphus garmani* and *Diaphus chrysorhynchus*. J. Fish. Biol. 82 (3), 1011–1031. https://doi.org/10.1111/jfb.12051.
Timmerman, C.A., Giraldo, C., Cresson, P., Ernande, B., Travers-Trolet, M., Rouquette, M., Denamiel, M., Lefebvre, S., 2021. Plasticity of trophic interactions in fish assemblages results in temporal stability of benthic-pelagic couplings. Mar. Environ. Res. 170. https://doi.org/10.1016/j.marenvres.2021.105412.
Tomás, J., Panfili, J., 2000. Otolith microstructure examination and growth patterns of *Vinciguerria nimbaria* (Photichthyidae) in the tropical Atlantic Ocean. Fish. Res. 46, 131–145. https://doi.org/10.1016/S0165-7836(00)00140-5.
Trueman, C.N., Johnston, G., O'Hea, B., MacKenzie, K.M., 2014. Trophic interactions of fish communities at midwater depths enhance long-term carbon storage and benthic production on continental slopes. Proc. R. Soc. B Biol. Sci. 281 (1787). https://doi.org/10.1098/rspb.2014.0669.
Tuset, V.M., Lozano, I.J., González, J.A., Pertusa, J.F., García-Díaz, M.M., 2003. Shape indices to identify regional differences in otolith morphology of comber, Serranus cabrilla (L., 1758). J. Appl. Ichthyol. 19 (2), 88–93.
Varghese, S.P., Somvanshi, V.S., Dalvi, R.S., 2014. Diet composition, feeding niche partitioning and trophic organisation of large pelagic predatory fishes in the eastern Arabian Sea. Hydrobiologia 736 (1), 99–114. https://doi.org/10.1007/s10750-014-1895-4.
Vipin, P.M., Pradeep, K., RaviI, R., Fernandez, T.J., Remasan, M.P., Madhu, V.R., Boopendranath, M.R., 2011. First estimate of the length–weight relationship of *Diaphus watasei* Jordan and Starks, 1904 Caught off the Southwest Coast of India. Asian Fish. Sci. 24 (4). https://doi.org/10.33997/j.afs.2011.24.4.010.
Wang, Y., Ma, C., Song, X., Li, M., Zhang, H., 2024. Assessment of fish diversity in the East China Sea hairtail national aquatic germplasm resources conservation zone using DNA barcoding. Glob. Ecol. Conserv. 53, e03013. https://doi.org/10.1016/J.GECCO.2024.E03013.
Wang, F., Wu, Y., Cui, Y., Chen, Z., Li, Z., Zhang, J., Zheng, S., 2019. δ13C and fatty acid composition of mesopelagic fishes in the South China Sea and their influence factors. Chem. Ecol. 35 (9), 788–804. https://doi.org/10.1080/02757540.2019.1651844.
Yamada, U., Tokimura, M., Horikawa, H., Nakabo, T., 2007. xxiv +. In: Fishes and Fisheries of the East China and Yellow Seas, 1. Tokai University Press, Hadano / Kanagawa, p. 262.
Zhang, C., Guo, H., 2024. Age, growth and feeding habit of Watases lanternfish *Diaphus watasei* (Pisces: Myctophidae) in the East China Sea. Fish. Sci. 90 (4), 555–564. https://doi.org/10.1007/s12562-024-01796-9.
Zhang, S., Jin, S., Zhang, H., Fan, W., Tang, F., Yang, S., 2016. Distribution of bottom trawling effort in the Yellow Sea and East China Sea. PLoS ONE 11 (11). https://doi.org/10.1371/journal.pone.0166640.
Zou, C., Yin, D., Wang, R., 2022. Mercury and selenium bioaccumulation in wild commercial fish in the coastal East China Sea: Selenium benefits versus mercury risks. Mar. Pollut. Bull. 180, 113754. https://doi.org/10.1016/J.MARPOL.